



# THE UNIVERSITY *of* EDINBURGH

## Edinburgh Research Explorer

### **Numerical modelling of transport time scales within Nador lagoon (Morocco)**

**Citation for published version:**

Borthwick, A, Jeyar, M, Chaabelasri, E, Salhi, N & Elmahi, I 2017, 'Numerical modelling of transport time scales within Nador lagoon (Morocco)' World Journal of Modelling and Simulation, vol. 13, no. 2.

**Link:**

[Link to publication record in Edinburgh Research Explorer](#)

**Document Version:**

Early version, also known as pre-print

**Published In:**

World Journal of Modelling and Simulation

**General rights**

Copyright for the publications made accessible via the Edinburgh Research Explorer is retained by the author(s) and / or other copyright owners and it is a condition of accessing these publications that users recognise and abide by the legal requirements associated with these rights.

**Take down policy**

The University of Edinburgh has made every reasonable effort to ensure that Edinburgh Research Explorer content complies with UK legislation. If you believe that the public display of this file breaches copyright please contact [openaccess@ed.ac.uk](mailto:openaccess@ed.ac.uk) providing details, and we will remove access to the work immediately and investigate your claim.



# Numerical modelling of transport time scales within Nador lagoon (Morocco)

Mohammed JEYAR<sup>1</sup>, Emiloud CHAABELASRI<sup>1,2</sup>, Najim SALHI<sup>2</sup>, Alistair G. L. BORTHWICK<sup>3</sup>, Imad ELMAHI<sup>2</sup>

<sup>1</sup>LME, Faculty of sciences. First Mohammed University, Morocco.

<sup>2</sup>National School of Applied Sciences, BP 03, Ajdir Al-Hoceima, First Mohammed University, Morocco.

<sup>3</sup>School of Engineering, The University of Edinburgh, The King's Buildings, Edinburgh EH9 3JL, UK.

## Abstract

An integrated 2D depth-averaged hydrodynamic dispersion model is used to simulate the time scales of tracer transport processes in the Nador lagoon, Morocco, for various tidal forcing conditions. Tidal hydrodynamics are predicted using a finite volume solver of the shallow water equations on an unstructured triangular mesh fitted to the lagoon geometry. Tracer dispersion is predicted by solving the Eulerian advection-diffusion equation. Residence and exposure times are determined from the remnant function obtained from the concentration of passive tracers released inside the lagoon. Numerical simulations covering spring and neap tidal cycles are used to investigate the influence of tidal forcing on residence and exposure times in sub-basins of the Nador lagoon, from which overall mean values of the time scales are estimated for the entire lagoon allowing for the return flow factor of the basin. The results demonstrate the importance of tidal cycles on transport time scales and self-cleansing of the Nador lagoon; for example, it is found that self-cleansing takes about 1 day longer at neap tide than at spring tide.

**Keywords:** Residence time; exposure time; hydrodynamical modeling, tracer transport, Nador lagoon.

## 1. Introduction

Many lagoons and gulfs are semi-enclosed basins from a hydrodynamic perspective. As coastal development occurs, human activities provide inputs that alter the trophic state and consequently the health of the ecosystems of such basins. After release into a coastal basin, the majority of contaminants, including nutrients, are transported in suspension or in solution (after dissolving in the seawater). The cleaning capacity of a coastal basin involves biogeochemical and physical processes, of which the latter is dominated by advection and diffusion. As a semi-enclosed basin flushes, water is transported to the open sea where it mixes with seawater. In practice, the efficiency of physical cleaning of a lagoon or gulf is expressed by the residence time of water particle within the basin. The cleaning capacity is in turn affected by water circulation within the basin, driven by tides, ocean swell, and (provided the basin is sufficiently large) Coriolis accelerations due to the Earth's rotation.

This paper considers the Nador Lagoon, which receives seawater from the Mediterranean Sea. In the Nador Lagoon, tidal forcing drives water circulation within the basin, and so its tidal characteristics control the lagoon's cleaning capacity. The flushing mechanism is produced through repeated exchange of the intertidal water volume between

the embayment (the Nador Lagoon) and the receiving water body of the Mediterranean Sea. Many recent investigations have studied the residence time of water particles in shallow semi-enclosed coastal basins. For example, Cucco et al. [1] computed the water residence time of the Venice lagoon using a 2D hydrodynamics model based on an advection-diffusion equation. Jain et al. [2] modelled residence and exposure times in the Pearl River Estuary, China, using a Lagrangian scheme to describe particle trajectories. Kenov et al. [3] calculated the residence time in the Mondego Estuary, Portugal using two methodologies: the first based on field data and a freshwater fraction model; and the second based on a Lagrangian transport model coupled to a two-dimensional hydrodynamic numerical model that solved depth-averaged advection and diffusion equations. Kenov et al. obtained similar results using the two methodologies.

The present study has two objectives. One is to describe a methodology by which to investigate the particle residence time in a coastal lagoon based on an Eulerian advection-diffusion approach [4]. The other is to assess the impact of tidal forcing on the residence and exposure times in certain sub-basins of the Nador lagoon, accounting for the return flow factor of the basin.

## **2. Materials and methods**

### *2.1. Site description*

The Nador lagoon is one of the largest lagoons in North Africa (115 km<sup>2</sup> area, 27 km long, and 7.5 km wide). The lagoon is located on the southern shore of the Mediterranean Sea, with the land side situated in a semiarid region (Figure 1). The lagoon complex may be divided into three domains as follows: a continental border region comprising salt marshes and rivers whose flows are characterised by irregular torrential runoff, but are dry most of the time; the Nador lagoon itself; and an island barrier broken by a single tidal inlet, Bokhana, through which exchange occurs with the sea. The external hydrodynamics of this coastal area depends on the tidal regime, littoral drift currents, and prevailing waves. The tidal regime of this Mediterranean region is microtidal and semidiurnal, the magnitude increasing toward the eastern inlet [5]. The internal hydrodynamics of the Nador lagoon is affected by: seawater entering the lagoon through an artificial inlet which is the dominant driving mechanism; hydrogeological contributions at the margins of the lagoon (See Figure 1); and surface water inputs arising from the periodic flows of ten small streams, most of which dry out completely in the summer causing freshwater discharges to be negligible relative to the tidal prisms. Of these streams, the Selouane is the most important, bringing urban/industrial waste effluent from Selouane village into the lagoon during the wet season.

### *2.2. Description of hydrodynamic model and dispersion model*

The Nador lagoon is shallow, of 7 m average depth. It is well mixed in the vertical direction, but its hydrographic parameters have large horizontal gradients. The shallow water approximations apply in this case where tidal wavelengths are very long compared to the depth of the lagoon, and tidal amplitudes are relatively small compared to both

wavelength and depth. By assuming the flow field is predominantly horizontal, vertical accelerations can be neglected, and pressure is hydrostatic; in keeping with the shallow water approximations, a two-dimensional depth-averaged hydrodynamic model has been developed to simulate current fields and investigate the associated forcing mechanisms [18]. Letting  $t$  be the time coordinate,  $x$  and  $y$  (m) the two horizontal Cartesian coordinates,  $U(x,y,t)$  and  $V(x,y,t)$  ( $\text{ms}^{-1}$ ) the respective depth-averaged flow velocity components,  $h(x,y,t)$  (m) the water depth,  $Z(x,y)$ (m) the non-erodible bottom elevation,  $h(x,y,t)+Z(x,y,t)$  the water surface elevation,  $g$  the acceleration due to gravity,  $\rho$  the water density, and  $\partial_t$  the partial derivative with respect to  $t$ , then the mass continuity equation and the respective  $x$ - and  $y$ -momentum equations are given by:

$$\partial_t(h) + \partial_x(hU) + \partial_y(hV) = 0 , \quad (1a)$$

$$\begin{aligned} \partial_t(hU) + \partial_x(hU^2 + \frac{1}{2}gh^2) + \partial_y(hUV) + \Omega V = -gh\partial_x(Z) + (\tau_{sx} - \tau_{bx})h^{-1} \\ + \nu_t(\partial_x^2 U + \partial_y^2 U) \end{aligned} , \quad (1b)$$

and

$$\begin{aligned} \partial_t(hV) + \partial_x(hUV) + \partial_y(hV^2 + \frac{1}{2}gh^2) - \Omega U = -gh\partial_y(Z) + (\tau_{sy} - \tau_{by})h^{-1} \\ + \nu_t(\partial_x^2 V + \partial_y^2 V) \end{aligned} , \quad (1c)$$

where  $\Omega$  is the Coriolis term;  $\nu_t$  is the depth-averaged turbulent kinematic viscosity;  $\tau_{bx}$  and  $\tau_{by}$  are the bed shear stresses determined empirically from  $\tau_{bx} = \rho c_f U \sqrt{U^2 + V^2}$  and  $\tau_{by} = \rho c_f V \sqrt{U^2 + V^2}$  where  $c_f = gn^2 h^{-1/3}$ , in which  $n$  is the Manning roughness coefficient;  $\tau_{sx}$  and  $\tau_{sy}$  are the surface shear stresses estimated empirically from  $\tau_{sx} = \rho_s C_D W^2 \cos \alpha$  and  $\tau_{sy} = \rho_s C_D W^2 \sin \alpha$  in which  $\rho_s$  is the air density,  $W$  is the wind speed at 10 m elevation, and  $C_D = (0.49 + 0.065W) 10^{-3}$  for  $W > 10$  m/s and  $1.14 \times 10^{-3}$  otherwise [21]; and  $\alpha$  is the angle between the wind direction and the  $x$ -coordinate. The turbulent kinematic viscosity is calculated using a simple algebraic eddy viscosity model,  $\nu_t = \alpha_t U^* h$ , in which  $U^* = \sqrt{c_f (U^2 + V^2)}$  is the maximum shear velocity, and  $\alpha_t$  is an empirical coefficient less than 1 [19, 20].

### 2.3. Residence and Exposure Times

The residence time of a lagoon, or segment of it, is often loosely referred to as the average time a water parcel or introduced substance remains within the system. The time period a water parcel, or substance, remains within a system depends on the location where and time when the water parcel is initially tagged or the substance is introduced [25, 26]. In the present study an Eulerian approach is used to estimate detailed spatial and temporal distributions of particle concentrations and the particle residence time. The Eulerian approach models the particulate phase as a continuum phase, and treats particulate matter

as passive pollutants. The simplicity of this approach arises from employing the advection-diffusion equation to compute the spatio-temporal distribution of particle concentrations. Relevant numerical models based on the Eulerian approach include [10], [11], [12], [13], [14] and [15].

Following Zimmerman [22], the residence time of a material element is defined by the time taken for this element to reach the outlet. Based on this concept, Takeoka [16, 17] introduced a remnant function to calculate the residence time, and defined the residence time as the time required for each element of the lagoon area to replace most of the mass of a conservative tracer, originally released, with new water. The tracer is subject to the action of the tidal currents that drive it out through the single inlet. This causes its concentration to decay. The remnant function  $r(t)$  of the concentration is given at each position of the domain as

$$r(x, y, t) = \frac{C(x, y, t)}{C_0} \quad (2)$$

where  $C(x, y, t)$  is the concentration at time  $t$  of the passive tracer in the  $x, y$  position, and  $C_0 = C(x, y, t = 0)$  is its initial value. The residence time  $\tau$  can then be defined according to Takeoka [16, 17] as:

$$\tau = \int_0^{\infty} r(t) dt ,$$

and for every position  $x, y$  of the domain as:

$$\tau(x, y) = \int_0^{\infty} r(x, y, t) dt .$$

The decay in concentration  $C$  is exponential, i.e.  $C(t) = C_0 \exp(-\alpha t)$ . Consequently, the residence time  $\tau$  can be computed as the time taken for the concentration to reduce to  $1/e$  of its initial value. A complete description of the model is given in [18].

To compute the water residence time in the Nador Lagoon, a passive tracer  $C$  is released in the lagoon basin, with an initial concentration corresponding to 100%. To simulate the behaviour of the tracer concentration, the model solves the following vertically-integrated advection-diffusion equation:

$$\frac{\partial C}{\partial t} - \frac{\partial UC}{\partial x} + \frac{\partial VC}{\partial y} = K_H \left( \frac{\partial^2 C}{\partial x^2} + \frac{\partial^2 C}{\partial y^2} \right) \quad (3)$$

where  $U$  and  $V$  are the depth-averaged flow velocity components and  $K_H$  is the horizontal eddy diffusivity. Fluxes through the lagoon bed and the water surface are neglected.

When a tide forces circulation, water mass from the lagoon is carried out of the embayment during the ebb phase. A certain fraction of the discharged water is lost by exchange and mixing within the receiving water body; the remainder returns back to the

lagoon basin during the subsequent flood phase. According to this definition, the residence time does not include the time interval spent by a water parcel when it re-enters the domain. Due to this limitation, another timescale, called the exposure time, has been introduced to measure the total amount of time spent by a water parcel in the control domain, noting all subsequent re-entries in the domain [23, 24]

#### 2.4. Numerical method

An existing, previously verified, numerical model, called 2-D Unstructured Finite Volume Shallow Water Model (UFV-SWM), is used to simulate the movement of the water free surface elevation, the hydrodynamic fluxes, and the transport diffusion of a tracer. The model uses unstructured meshes, and incorporates upwinded numerical fluxes and slope limiters in a Godunov-type finite volume scheme to provide sharp resolution of steep bathymetric gradients that may develop in the approximate solution. The scheme is non-oscillatory and possesses the conservation property (important for conserving pollutant mass during the transport process). UFV-SWM has been widely used to simulate shallow flows in open channels, rivers, and coastal waters. For a more detailed description of UFV-SWM the reader is referred to [6], [7], [8], and [9].

##### 2.4.1. Input data and boundary conditions

The numerical computation was carried out on an unstructured finite volume grid composed of 8075 triangular elements and 14042 nodes. The bathymetry of the Nador lagoon, obtained by combining several datasets, was interpolated onto the grid.

The principal hydraulic forcing of the Nador lagoon is tidal. At the open boundary, the water depth was therefore prescribed according to a mean value  $h_0$  and a fluctuating-free surface elevation  $h_f$  such that  $h(t) = h_0 + h_f$ , where  $h_f$  depends on the given tidal components as follows,

$$h_f = \sum_{i=1} A_i \cos(\omega_i t + \phi_i), \quad (4)$$

where  $A_i$  is the wave amplitude,  $\omega_i$  is the angular frequency and  $\phi_i$  is the tide phase of the  $i$ -th tidal component. Values for these parameters were determined from global observation tidal values, which included the semi-diurnal tidal component  $M_2$ . All other boundaries were assumed to be solid wall without wetting drying.

To calculate the residence time, two different boundary conditions for the concentration tracer were applied at inlet nodes. For water exiting the lagoon, a transmissive boundary condition was applied to the tracer concentration. For water entering the lagoon, the concentration at the open boundary nodes was set to zero, assuming that the incoming tide contains clean water.

Initially, water conditions in the lagoon are still, and so the tracer was distributed uniformly throughout the lagoon, such that:

$$C_0(x, y) = C(x, y, t = 0) = 1. \quad (5)$$

Table 1 lists the selected values of key parameters used as input by the numerical model. Tidal forcing was solely considered; other meteorological forcing mechanisms, such as wind pressure and heat flux were neglected.

### **3. Numerical investigation and discussions**

#### *3.1. Model setup*

In order to calibrate the numerical model for calculation of residence and exposure times, the model was run against 14 sets of observed sea level measurements (see table 2 and figure 2) for each time scale, provided by the Moroccan Ministry of Equipment, Transport and Logistics, and covering the winter and spring periods of the year 2014 (see figure 2). Seven data sets were collected during spring tides and seven data sets during neap tides. Freshwater input at inlet nodes for these data sets covered both ebb and flood tides, and high and low water levels. The numerical scenarios, corresponding to neap and spring cases, commenced at high water with each following scenario delayed by two hours from the previous. In all cases, the model was run firstly for three tidal cycles with freshwater discharge conditions in order to approach limit cycle conditions, before results were recorded, the aim being to minimize transient effects arising from the initial conditions. After spin up, the model was run for a further 40 days to investigate numerically the impact of tidal forcing on residence and exposure times.

#### *3.2. Remnant functions*

Figure 3 illustrates the temporal variation of the remnant functions for residence and exposure times. Both remnant functions decrease almost monotonically with an oscillatory component superimposed due to the tidal fluctuation. The remnant function of exposure time has a value always larger than that of the return flow, because the fraction of re-entering water, corresponding to the flood water phase, has been taken into account.

#### *3.3. Simulated residence and exposure times*

In order to understand the influence of tides on residence and exposure times in the whole Nador lagoon, the basin has been divided into three major sub-basins, each allocated the same hydrodynamic characteristics: water depth, tidal current, and boundary conditions. The sub-basins are namely, from the north to the south, NB, CB and SB. The NB and SB sub-basins are the least exposed to tidal currents owing to their being located large distances from the lagoon inlet and potentially having the largest time scale values.

For both tidal phases, neap and spring, the predicted time scales in NB have high values, with the maximum value of residence time reaching 15.16 days during spring tide and a maximum value of exposure time reaching 24.35 days during neap tide. For both spring and neap tide simulations the largest discrepancies in average water residence times occur in the NB sub-basin. Differences in exposure time between the spring and neap simulations are found to be about 1.48 days for SB and 2.65 days for NB. Note that these

results do not incorporate the effect of movement of the released tracer, however this does not strongly affect the estimates of average time scales of the basin and sub-basins.

#### 3.4. *Spatial distribution of residence and exposure times*

Figure 4 plots spatial distributions of residence time and exposure time obtained during spring and neap tides, obtained by averaging the results from the whole set of seven simulations in each case. Both distributions are quite heterogeneous, dominated by relatively large values which range from < 1 day inside the inlet to > 40 days in the inner lagoon. The residence and exposure times are consistently < 32 days throughout the lagoon, except for certain northern regions. The average values of the residence and exposure times computed for the whole basin can be divided into three ranges according to the division into sub-basins. Residence and exposure times of 12 days and 20 days are obtained for the neap-spring tide cases in CB. The exposure and residence times in NB and SB are generally greater than for CB. Qualitatively, the spatial distributions of residence time and exposure time in Nador lagoon are primarily dependent on the distance from the inlet and the overall basin geometry.

#### 3.5. *Return flow factor*

Further analysis was carried out to understand better the influence of the tidal forcing and contribution of returning water on the time scales computation. To achieve this, the return flow factor  $R_{ff}$  was calculated for each sub-element in the lagoon domain. The return flow factor indicates the fate of the concentration once it is outside the embayment. The value  $R_{ff} = 0$  expresses the fact that no water previously ejected returns into the lagoon and  $R_{ff} = 1$  corresponds to a situation where all tracer returns to the basin. The return flow factor provides another way to estimate the average residence time in a small and well-mixed embayment; it depends on three important factors, as outlined by Sanford et al. [27]: the phase of the tidal flow in the connecting channel relative to the flow along the coast; the degree of mixing that occurs once the water is outside the embayment; and the strength of the inlet flow relative to the strength of the coastal current. The return flow factor  $R_{ff}$  is defined [1]:

$$R_{ff} = 1 - \frac{R_T}{E_T} \quad (6)$$

in which  $R_T$  is the predicted residence time and  $E_T$  is the predicted exposure time. Figure 5 shows the spatial distribution of  $R_{ff}$ . In general, the value of the return flow factor is about 0.5, and does not exceed 0.59 for a neap tide or 0.54 for a spring tide. This indicates that about half of the exposure time is associated with the returning water. The results imply that tidal variability has relatively small influence on the values of the timescales throughout the basin.

#### 3.6. *Conclusion*



This paper has described application of a depth-integrated 2D shallow flow model to predict the residence time and exposure time due to tidal forcing in the Nador Lagoon. A remnant function method was employed to quantify the spatially varying transport mechanism of a dissolved substance and hence compute the mean time scales of the Nador lagoon. This was accomplished by using a high-resolution mass-preserving hydrodynamic and mass-transport model. The residence times, as computed, do not provide an exact value that characterizes the water of a specific location, but can be considered a valid time scale that characterizes the transport processes in the lagoon basin, and also an estimate of the relative efficiency of the renewal capacity of the basin. Furthermore, the exact time at which a tracer is released in a tidal phase affects the values of both the residence time and exposure time in the Nador lagoon. If the tracer is released at the neap tide, it will stay in the lagoon for a much longer time (approximately 1 day) than that released at the spring tide. The difference between the residence and exposure time could be used to trigger countermeasures to control contaminants from re-entering the lagoon.

## References

- [1] Cucco, A. and Umgiesser, G., Modeling the Venice Lagoon residence time. *Ecological Modelling*. **193**(1): 34-51 (2006).
- [2] Sun, J., Lin, B., Li, K. and Jiang, G., A modelling study of residence time and exposure time in the Pearl River Estuary, China. *Journal of Hydro-environmental Research*, **8**(3): 281-291 (2014).
- [3] Kenov, I.A., Garcia, A.C. and Neves, R., Residence time of water in the Mondego estuary (Portugal). *Estuarine, Coastal and Shelf Science*, **106**: 13-22 (2012).
- [4] Chang, T.-J., Kao, H.-M. and Yam, R.S.-Y., Lagrangian modeling of the particle residence time in indoor environment. *Building and Environment*, **62**: 55-62 (2013).
- [5] Brethes, J.C. and Tesson, M., Observations hydrologiques sur la Sebkhia Bou Areg (Lagune de Nador, Maroc). Bilan d'automne 76 et d'hiver 77, Trav. Doc. Pêches Maroc, N° 24, Casablanca, (1978) 17 pp.
- [6] Benkhaldoun, F., Elmahi, I. and Seaid, M., Application of mesh-adaptation for pollutant transport by water flow. *Mathematics and Computers in Simulation*. **79**(12): 3415-3423 (2009).
- [7] Benkhaldoun, F., Elmahi, I. and Seaid, M.A., new finite volume method for flux gradient and source-term balancing in shallow water equations. *Computer Methods in Applied Mechanics and Engineering*, **199**(49-52): 3324-3335 (2010).

- [8] Chaabelasri, E.M., Amahmouj, A., Jeyar, M., Borthwick, A. G. L., Salhi, N. and Elmahi, I. Numerical survey of contaminant transport and self-cleansing of water in Nador Lagoon. Morocco. *Modelling and Simulation in Engineering*, Article ID 179504, 8 pages. doi:10.1155/2014/179504 (2014).
- [9] Chaabelasri, E.M., Borthwick, A.G.L., Salhi, N. and Elmahi, I. Balanced adaptive simulation of pollutant transport in Bay of Tangier (Morocco). *World Journal of Modelling and Simulation*, **10**(1): 3-19 (2014).
- [10] Zhao, B., Zhang, Y., Li, X., Yang, X. and Huang, D. Comparison of indoor aerosol particle concentration and deposition in different ventilated rooms by numerical method. *Building and Environment*, **39**(1): 1-8 (2004).
- [11] Awbi, H.B. *Ventilation of Buildings*. Chapman and Hall, London (1991).
- [12] Bady, M., Kato, S. and Huang, H. Towards the application of indoor air ventilation efficiency indices to evaluate the air quality of urban areas. *Building and Environment*, **43**(12): 1991-2004 (2008).
- [13] Danckwerts, P.V., Continuous flow systems: distribution of residence times. *Chemical Engineering Science*, **2**(1): 1-18 (1953).
- [14] Agmon, N., The residence time equation. *Chemical Physics Letters*, **497**(4): 184-6 (2010).
- [15] Ghirelli, F. and Leckner, B., Transport equation for the local residence time of a fluid. *Chemical Engineering Science*, **59**: 513-523 (2004).
- [16] Takeoka, H., Exchange and transport time scales in the Seto Inland Sea. *Continental Shelf Research*, **3** (4): 327-341 (1984).
- [17] Takeoka, H., Fundamental concepts of exchange and transport timescales in a coastal sea. *Continental Shelf Research*, **3**(3): 311-326 (1984).
- [18] Luettich Jr., R.A., Carr, S.D., Reynolds-Fleming, J.V., Fulcher, C.W. and McNinch, J.E., Semi-diurnal seiching in a shallow, micro-tidal lagoonal estuary. *Continental Shelf Research*, **22**(11-13): 1669-1681 (2002).
- [19] Wu, W., Depth-averaged two-dimensional numerical modeling of unsteady flow and nonuniform sediment transport in open channels. *Journal of Hydraulic Engineering, ASCE*, **130**(10): 1013-1024 (2004).

- [20] Colombini, M. and Stocchino, A., Wind effect in turbulence parametrization. *Advances in Water Resources*, 28(9): 939-949 (2005).
- [21] Large, W.G. and Pond, S., Open ocean momentum flux measurements in moderate to strong winds. *Journal of Physical Oceanography*, **11**: 324-336 (1981).
- [22] Zimmerman, J.T.F., Mixing and flushing of tidal embayments in the Western Dutch Wadden Sea, Part I: Distribution of salinity and calculation of mixing timescales. *Netherlands Journal of Sea Research*, **10**(2): 149-191 (1976).
- [23] Delhez, E.J.M., Transient residence and exposure times. *Ocean Science*, **2**: 1-9 (2006).
- [24] Delhez, E.J.M., Heemink, A.W. and Deleersnijder, E., Residence time in a semi-enclosed domain from the solution of an adjoint problem. *Estuarine, Coastal and Shelf Science*, **61**(4): 691-702 (2004).
- [25] van de Kreeke, J., Residence time: application to small boat basins. *ASCE Journal of Waterway, Port, Coastal and Ocean Engineering Division*, **109**(4): 416-428 (1983).
- [26] Prandle, D.A., A modelling study of the mixing of  $^{137}\text{Cs}$  in the seas of the European continental shelf. *Philosophical Transactions of the Royal Society, London, Series A*, **310**(1513): 407-436 (1984).
- [27] Sanford, L.P., Boicourt, W.C. and Rives, S.R., Model for estimating tidal flushing of small embayments. *Journal of Waterway, Port, Coastal and Ocean Engineering, ASCE*, **118**(6): 635-654 (1992).

## Tables

Table 1: Hydrodynamic model parameters.

| Parameter                                      | Symbol     | Value   |
|--|------------|---|
| Water density                                  | $\rho_w$   | 1025 kg.m <sup>-3</sup>                       |
| Air density                                    | $\rho_a$   | 1.225 kg.m <sup>-3</sup>                      |
| M <sub>2</sub> tide (spring / neap) amplitudes | $A$        | 0.35 / 0.26 m                                 |
| Tide angular frequency                         | $\omega$   | 1.3631 x 10 <sup>-4</sup> rad.s <sup>-1</sup> |
| Tide phase                                     | $\varphi$  | 45 <sup>o</sup>                               |
| Time step                                      | $\Delta t$ | ~ 3 s   |
| Maximum area of mesh cell                      |            | 48000 m <sup>2</sup>                          |
| Minimum area of mesh cell                      |            | 450 m <sup>2</sup>                            |

Table 2: Model scenario runs for evaluating residence time and exposure time for Nador lagoon .

| Tidal  |       | Runs     |                 | Maximum tide range [m] | Average period [h] |
|--------|-------|----------|-----------------|------------------------|--------------------|
| Type   | phase | Names    | Times           |                        |                    |
| Neap   | High  | Run-N0h  | $t_{N0h}$       | 00.64<br>-             | 12.48              |
|        |       | Run-N2h  | $t_{N0h} + 2h$  |                        |                    |
|        |       | Run-N4h  | $t_{N0h} + 4h$  |                        |                    |
|        | Low   | Run-N6h  | $t_{N0h} + 6h$  |                        |                    |
|        |       | Run-N8h  | $t_{N0h} + 8h$  |                        |                    |
|        |       | Run-N10h | $t_{N0h} + 10h$ |                        |                    |
|        |       | Run-N12h | $t_{N0h} + 12h$ |                        |                    |
| Spring | High  | Run-S0h  | $t_{S0h}$       | 00.52<br>-             | 12.14              |
|        |       | Run-S2h  | $t_{S0h} + 2h$  |                        |                    |
|        |       | Run-S4h  | $t_{S0h} + 4h$  |                        |                    |
|        | Low   | Run-S6h  | $t_{S0h} + 6h$  |                        |                    |
|        |       | Run-S8h  | $t_{S0h} + 8h$  |                        |                    |
|        |       | Run-S10h | $t_{S0h} + 10h$ |                        |                    |
|        |       | Run-S12h | $t_{S0h} + 12h$ |                        |                    |

Table 3: Simulated values of the residence time and exposure time for the whole Nador lagoon and its sub-basins during neap and spring tide.

| Tidal(Type-phase)  | Residence times [D] |       |       |       | Exposure times [D] |       |       |       |
|--------------------|---------------------|-------|-------|-------|--------------------|-------|-------|-------|
|                    | Whole basin         | NB    | CB    | SB    | Whole basin        | NB    | CB    | SB    |
| Neap tide (days)   | 05,63               | 13,68 | 4,335 | 11,49 | 13,12              | 24,35 | 10,96 | 20,53 |
| Spring tide (days) | 06,08               | 15,16 | 04,57 | 12,46 | 11,50              | 21,66 | 9,377 | 17,91 |

Table 4: Simulated return flow factor for the whole Nador lagoon and its sub-basins during neap and spring tide.

| Scenario    | Whole basin | NB   | CB    | SB   |
|-------------|-------------|------|-------|------|
| Spring tide | 0,57        | 0,43 | 0,60  | 0,44 |
| Neap tide   | 0,47        | 0,30 | 0,512 | 0,30 |

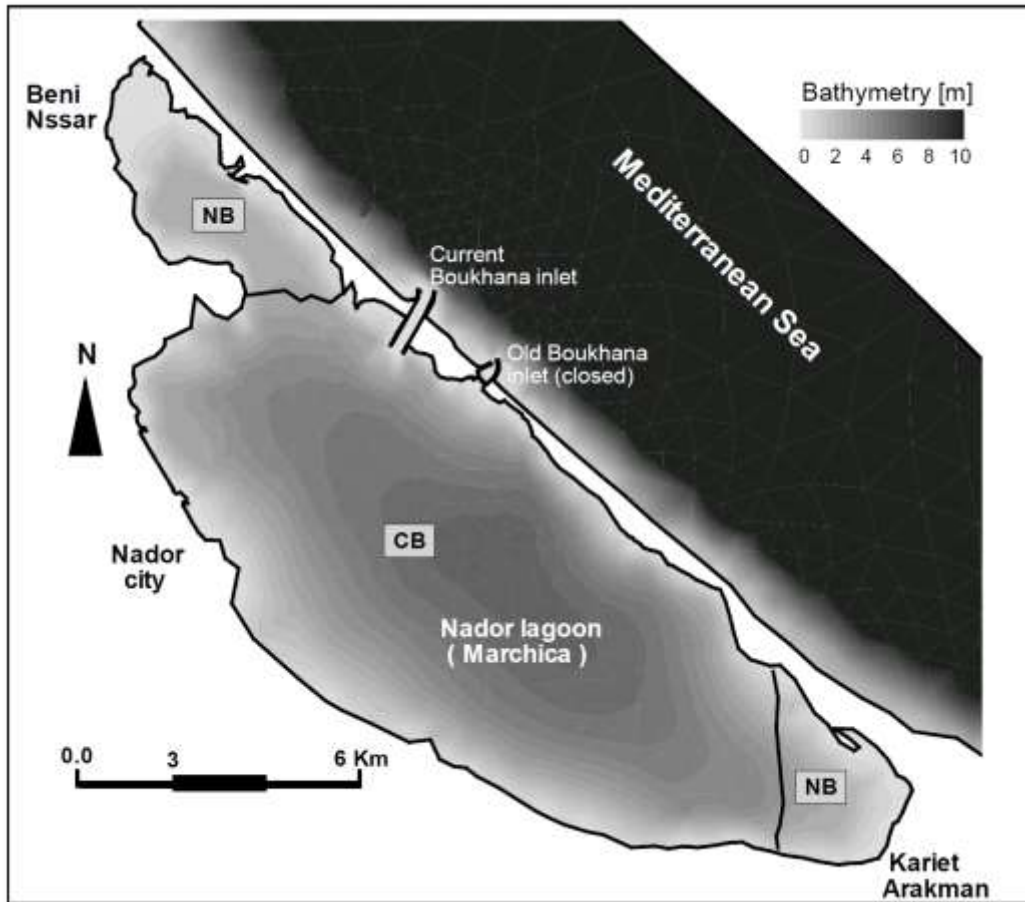


Figure 1: Map of the Nador Lagoon showing the Boukhana inlet location and the bathymetry. The map illustrates partition of the lagoon basin into three regions: the north sub-basin (NB); the central sub-basin (CB); and the southern sub-basin (SB).

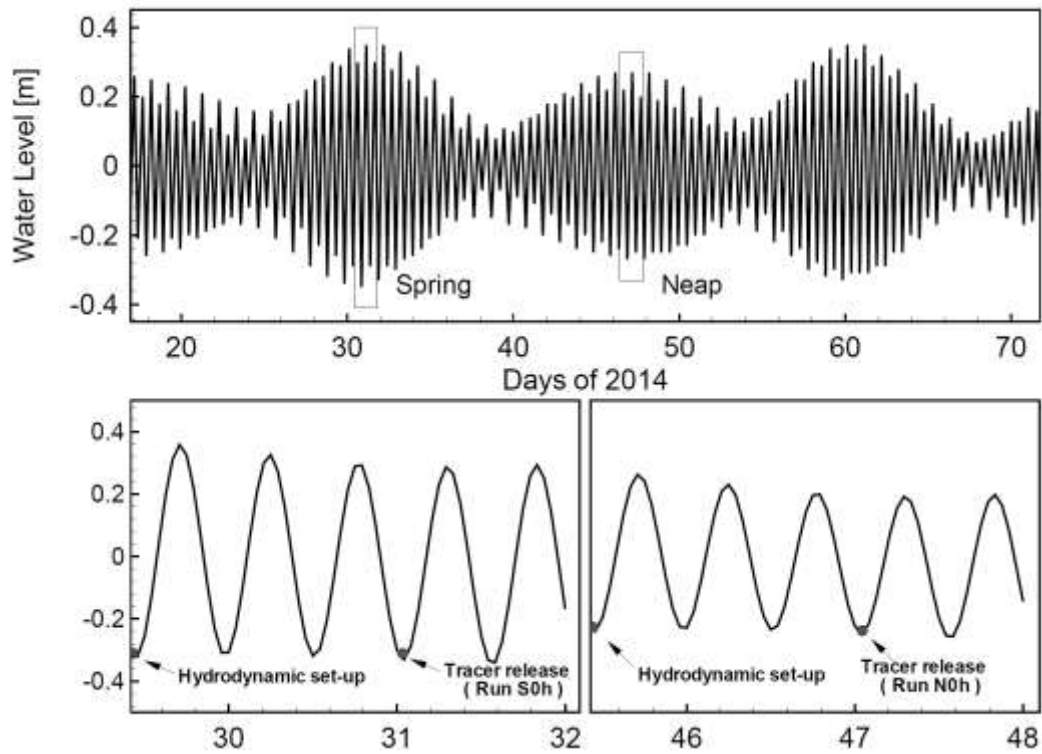


Figure 2: Water level time histories at a location near the inlet inside the lagoon over several spring-neap cycles in 2014. The lower inset plots focus on detailed tidal cycles at the spring and neap tides (indicated in the upper plot by rectangles) with the hydrodynamic setup time and first tracer release run time indicated by arrows.

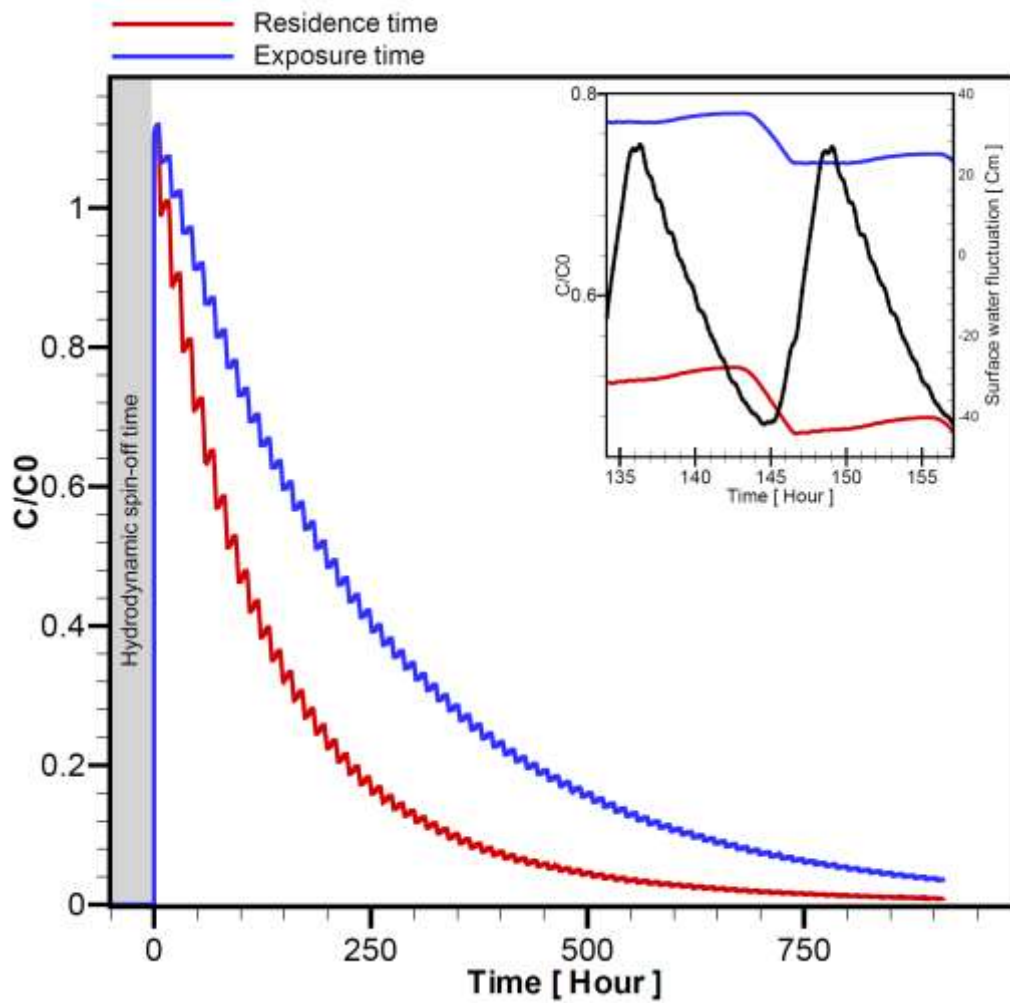


Figure 3: Remnant functions of residence and exposure times over 900 hours; the inset shows the effect of individual semi-diurnal tidal cycles on the remnant functions.



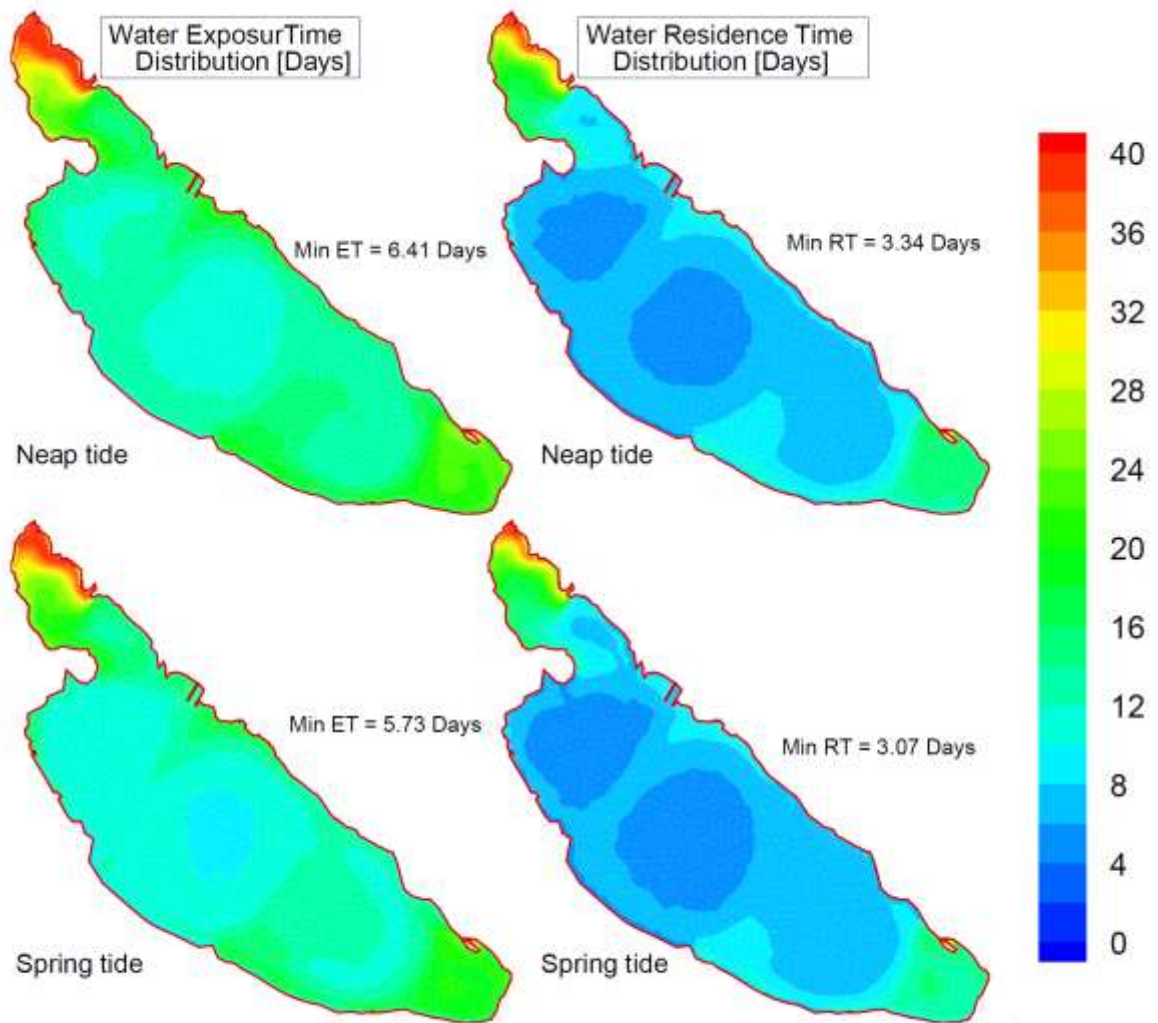


Figure 4: Water residence time and exposure time distributions in the Nador Lagoon during neap and spring tides.

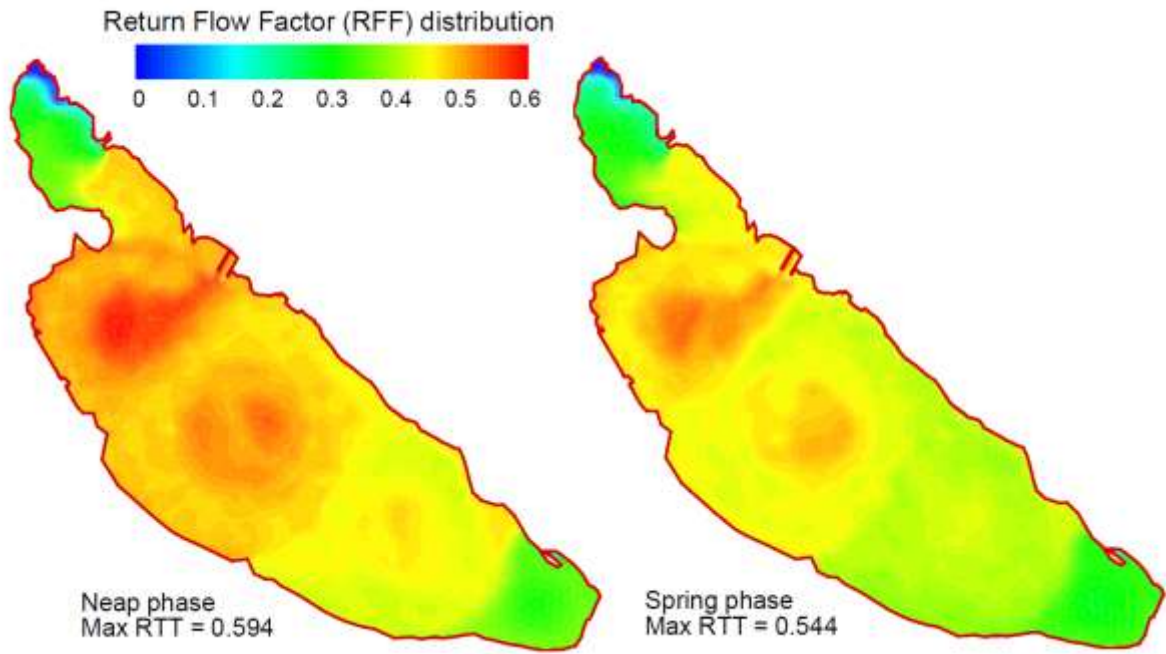


Figure 5: Return Flow Factor distributions in the Nador Lagoon during spring and neap tide phases.